Modern Physics Letters A

DETERMINATION OF CHARM QUARK MASS AND $\alpha_s(M_Z)$ FROM HERA DATA

AMANDA COOPER-SARKAR

Dept. of Physics, University of Oxford,Keble Rd, OXFORD, OX1 3RH, UK
email:a.cooper-sarkar1@physics.ox.ac.uk

Received (24 May 2013)
Revised ()

Charm production data from HERA may be used to determine the charm quark mass and jet production data from HERA may be used to detrmine $\alpha_s(M_Z)$. Recent results are summarised.

1. Introduction

HERA was an electron(positron)-proton collider located at DESY, Hamburg. It ran in two phases HERA-I from 1992-2001 and HERA-II 2003-2007. Two similar experiments, H1 and ZEUS, took data. In HERA-1 running each experiment collected $\sim$ 100pb^{-1} of e^+p data and $\sim$ 15pb^{-1} of e^-p data with electron beam energy 27.5GeV and proton beam energies 820, 920 GeV. In HERA-II running each experiment took $\sim$ 140pb^{-1} of e^+p data and $\sim$ 180pb^{-1} of e^-p data with the same electron beam energy and proton beam energies 920 GeV.

Deep inelastic lepton-hadron scattering data has been used both to investigate the theory of the strong interaction and to determine the momentum distributions of the partons within the nucleon. The data from the HERA collider now dominate the world data on deep inelastic scattering since they cover an unprecedented kinematic range: in Q^2, the (negative of the) invariant mass squared of the virtual exchanged boson, $0.045 < Q^2 < 3 \times 10^{-5}$; in Bjorken x, $6 \times 10^{-7} < x < 0.65$. Futhermore, because the HERA experiments investigated e^+p and e^-p, charge current(CC) and neutral current (NC) scattering, information can be gained on flavour separated up- and down-type quarks and antiquarks and on the gluon- from its role in the scaling violations of perturbative quantum-chromo-dynamics. The formalism of how the deep inelastic cross sections relate to the parton distributions though the QCD-improved parton model, and how parton didtribution functions are then extracted from the data, is well documented (see for example ref. [1]) and only a brief description of the HERAPDF formalism will be given here. This contribution concentrates on results of relevance for the fundamental parameters of QCD: $\alpha_s(M_Z)$ and the charm qurak mass m_c.

2. HERAPDF Formalism

Perturbative QCD predicts the Q^2 evolution of the parton distributions, but not the x dependence. Parton distributions are extracted by performing a direct numerical integration of the DGLAP evolution equations at NLO. A parametrised analytic shape for the parton distributions is assumed to be valid at some starting value of $Q^2 = Q_0^2$. For the HERAPDF the value $Q_0^2 = 1.9$ GeV^2 is chosen such that the starting scale is below the charm mass threshold, $Q_0^2 < m_c^2$. Then the DGLAP equations are used to evolve the parton distributions up to a different Q^2 value, where they are convoluted with NLO coefficient functions to make predictions for the structure functions. The heavy quark coefficient functions are usually calculated in the general-mass variable-flavour-number scheme of Thorne [2]. However, for the study of the charm mass various other schemes have been considered, see Section 3.1 The heavy quark masses for the central HERAPDF fits were chosen to be $m_c = 1.4$ GeV and $m_b = 4.75$ GeV and the strong coupling constant was fixed to $\alpha_s(M_Z) = 0.1176$. (The values of m_c and $\alpha_s(M_Z)$ are varied when studies of these parameters are performed.) The predictions are then fitted to the combined HERA data sets for NC and CC e^+p and e^-p scattering. A minimum Q^2 cut of $Q^2_{min} = 3.5$ GeV^2 was imposed to remain in the kinematic region where perturbative QCD should be applicable.

The fit parameters are those necessary to specify the input analytic shape. The valence quark distributions xu_v, xd_v, and the u-type and d-type anti-quark distributions $x\bar{U}$, $x\bar{D}$ ($x\bar{U} = x\bar{u}$, $x\bar{D} = x\bar{d} + x\bar{s}$) are parametrised at the input scale $Q_0^2 = 1.9$GeV^2 by the generic form

$$xf(x) = Ax^B(1-x)^C(1 + Dx + Ex^2). \quad (1)$$

The parametrisation for the gluon distribution xg can be extended, to include a term $-A_{g'}x^{B_{g'}}(1-x)^{C_{g'}}$, such that the NLO gluon may become negative at low x and low Q^2 (however it does not do so in the kinematic region of the HERA data). The normalisation parameters, A_g, A_{u_v}, A_{d_v}, are constrained by the quark number sum-rules and momentum sum-rule. Constraints are imposed to ensure that $\bar{u} = \bar{d}$ at low-x, and to specify the strangeness fraction in the sea. The full details for all HERAPDFs are given in ref. [1]

The experimental uncertainties on the HERAPDF are determined using the conventional χ^2 tolerance, $\Delta\chi^2 = 1$, for 68%C.L. However model uncertainties and parametrisation uncertainties are also considered. The choice of the heavy quark masses is varied, the choice of Q^2_{min} is varied and the strangeness fraction is varied. Parametrisation variations for which the E and the D parameters for all the PDFs are freed are considered and variation of the starting scale Q_0^2 in the range, $1.5 < Q_0^2 < 2.5$GeV^2, is also considered. These model and parametrisation uncertainties are an integral part of the HERAPDF uncertainties.

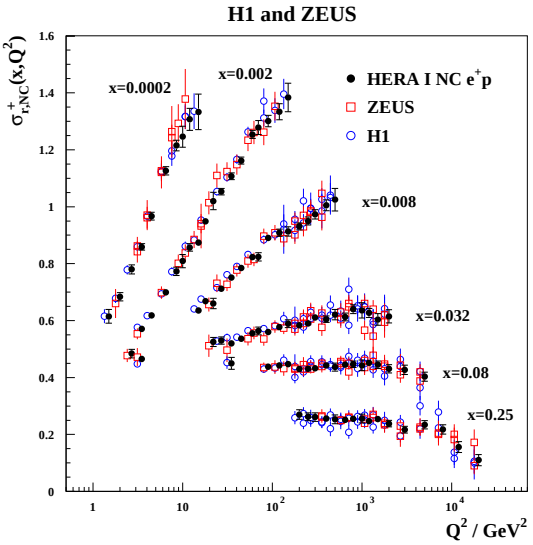

Fig. 1. HERA combined NC e^+p reduced cross section as a function of Q^2 for six x-bins compared to the separate H1 and ZEUS data input to the averaging procedure. The individual measurements are displaced horizontally for a better visibility.

3. Results

From 2008, the H1 and ZEUS experiments began to combine their data in order to provide the most complete and accurate set of deep-inelastic data as the legacy of HERA. Data on inclusive cross-sections have been combined for the HERA-I phase of running [3] and a preliminary combination has been made also using the HERA-II data [5]. HERA-jet data have been added to this combination in order to give more information on $\alpha_s(M_Z)$ and the gluon distribution [8]. Very recently a combination of data on $F_2^{c\bar{c}}$ has been used to give information on the charm quark mass [4].

The combination of the H1 and ZEUS data sets takes into account the full correlated systematic uncertainties of the individual experiments such that the total uncertainty of the combined measurement is typically smaller than 2%, for $3 < Q^2 < 500$ GeV^2, and reaches 1%, for $20 < Q^2 < 100$ GeV^2. In Fig 1 averaged data are compared to the input H1 and ZEUS data, illustrating the improvement in precision. Because of the reduction in size of the systematic error this improvement is far better than would be expected simply from the rough doubling of statistics which combining the two experiments represents.

A combination has also been made of data on $F_2^{c\bar{c}}$ [4] from various different methods of tagging charm: using the D^*, using the vertex detectors to see the displaced decay vertex, using direct D_0, D^+ production identified using the vertex detectors, and indentifying semi-leptonic charm decays via muons, also using the vertex detectors.

The results of the $F_2^{c\bar{c}}$ combination compared to the separate measurements

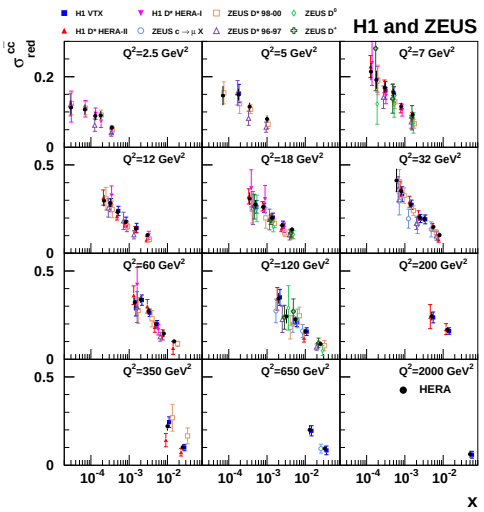

Fig. 2. The HERA combined measurement of $F_2^{c\bar{c}}$ compared to the data sets of H1 and ZEUS used for the combination. these data sets are slightly displaced in x for visibility.

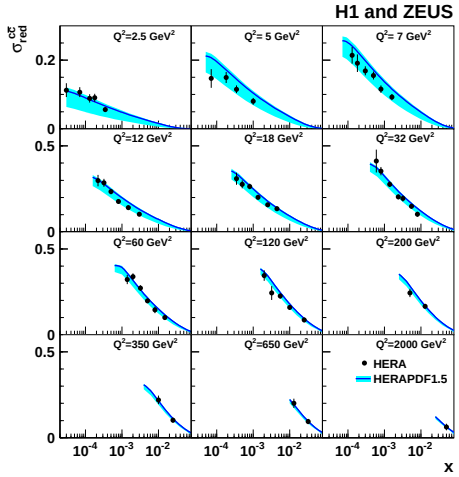

Fig. 3. The HERA combined measurement of $F_2^{c\bar{c}}$ compared to the predictions of HERAPDF1.0

which went into it are shown in Fig 2. The $F_2^{c\bar{c}}$ combination is shown compared to the predictions of HERAPDF1.0 in Fig. 3.

3.1. *Charm quark mass*

The uncertainty bands on these predictions are dominated by the variation of the charm quark mass, $1.35 < m_c < 1.65$GeV, used for the model uncertainty. The combined $F_2^{c\bar{c}}$ data can help to reduce this uncertainty. Fig. 4 (top left) compares the χ^2, as a function of the charm mass, for a fit which includes charm data to that

for the HERAPDF1.0 fit which does not use these data, when using the Thorne-Roberts (RT) variable-flavour-number (VFN) scheme. The charm data have a clear preference for a particular charm quark mass. However, the RT heavy flavour VFN scheme is not unique, specific choices are made for threshold behaviour. In Fig. 4 (top right) the χ^2 profiles for the standard and the optimized versions (optimized for smooth threshold behaviour) of this scheme are compared. The same figure also compares the alternative ACOT VFN schemes and the Zero-Mass VFN scheme. Each of these schemes favours a different value for the charm quark mass, and the fit to the data is good for all the heavy-quark-mass schemes considered.

Each of the VFN schemes has been used to predict W and Z production for the LHC and their predictions for W^+ are shown in Fig. 4 (bottom left) as a function of the charm quark mass. If a particular value of the charm mass is chosen then the spread of predictions is as large as $\sim 7\%$. However this spread is considerably reduced $\sim 1\%$ if each heavy quark scheme is used at its own favoured value of the charm quark-mass. Furher details of this study are given in ref. [4].

It is important to note that the schemes so far considered are General Mass VFN Schemes and that the charm quark mass used in such schemes is the pole-mass. However since the since the relationship between the pole-mass and the running-mass (or MSbar mass) does not converge it is better to use the running-mass. This has been done within the Fixed Flavour Number scheme [6] and the result is $m_c(m_c) = 1.26 \pm 0.05$ as shown in Fig. 4 (bottom right).

3.2. $\alpha_s(M_Z)$

The value of $\alpha_s(M_Z)$ is strongly correlated to the gluon PDF shape in fits to inclusive DIS data, because the gluon PDF is determined indirectly from the scaling violations. Jet production cross-sections depend directly on the gluon PDF. This extra information reduces the strong correlation between the gluon and $\alpha_s(M_Z)$ and allows competitive measurements of $\alpha_s(M_Z)$. Such studies have been made using jet data alone and by making a simultaneous fit of PDFs and $\alpha_s(M_Z)$.

Two recent studies using jet data alone are reported here. The first uses H1 normalised inclusive jet, di-jet and tri-jet cross-sections [9] which are well described by NLO QCD predictions from NLOJet++ [10] using CT10 PDFs [11] with $\alpha_s(M_Z) = 0.118$, see Fig. 5. A regularized unfolding is performed for all bins and multijet categories simultaneously to correct for detector effects and this yields a complete correlation matrix, which is used when these data are included into QCD fits which fix the PDF used (CT10 PDF) while varying $\alpha_s(M_Z)$. The covariance matrix was used to normalize the different jet rates to the inclusive neutral-current DIS cross section. This normalization reduces both the experimental and the theoretical uncertainties. Values of $\alpha_s(M_Z)$ are extracted separately from inclusive jets, di jets and tri-jets samples yielding:

$\alpha_S(M_Z) = 0.1197 \pm 0.0008$ (exp.) $\pm$ 0.0014 (PDF) $\pm$ 0.0011 (hadr.) $\pm$ 0.0053 (th.) for inclusive jets

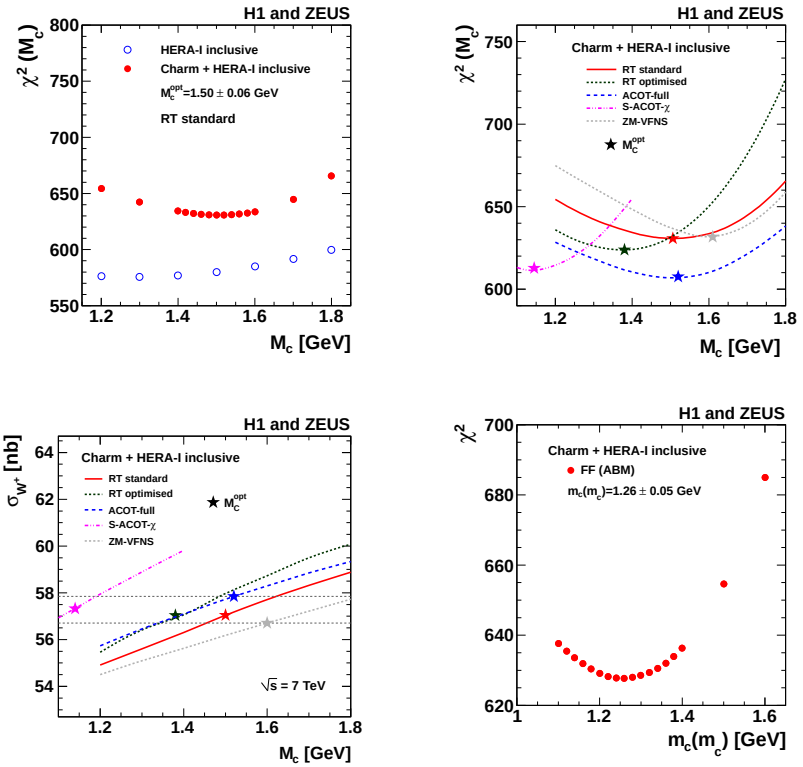

Fig. 4. The χ^2 of the HERAPDF fit as a function of the charm mass parameter m_c^{model}. Top left; using the RT-standard heavy-quark-mass scheme, when only inclusive DIS data are included in the fit and when the data for $F_2^{c\bar{c}}$ are also included in the fit. Top right; using various heavy-quark-mass schemes, when the data for $F_2^{c\bar{c}}$ are also included in the fit. Bottom left; predictions for the W^+ cross-sections at the LHC, as a function of the charm mass parameter m_c^{model}, for various heavy-quark-mass schemes. Bottom right: Using the FFN scheme in terms of the running mass $m_c(m_c)$.

$\alpha_S(M_Z) = 0.1142 \pm 0.0010$ (exp.) $\pm$ 0.0016 (PDF) $\pm$ 0.0009 (hadr.) $\pm$ 0.0048 (th.) for dijets and

$\alpha_S(M_Z) = 0.1185 \pm 0.0018$ (exp.) $\pm$ 0.0013 (PDF) $\pm$ 0.0016 (hadr.) $\pm$ 0.0042 (th.) for tri-jets.

There is some tension between the di-jet and inclusive jet measurements, possibly due to missing higher order calculations, so that to make a combined $\alpha_s(M_Z)$ extraction the cross-section predictions at NLO and LO were required to agree within 30%. This was fulfilled for 42 out of 65 bins. The combined fit then gives

$\alpha_S(M_Z) = 0.1163 \pm 0.0011$ (exp.) $\pm$ 0.0014 (PDF) $\pm$ 0.0008 (hadr.) $\pm$ 0.0039 (th.),

where the largest uncertainty is the theoretical uncertainty from scale variation.

The second study uses ZEUS photoproduction data, where a quasi-real photon is emitted from the incoming lepton. In direct photoproduction, the photon

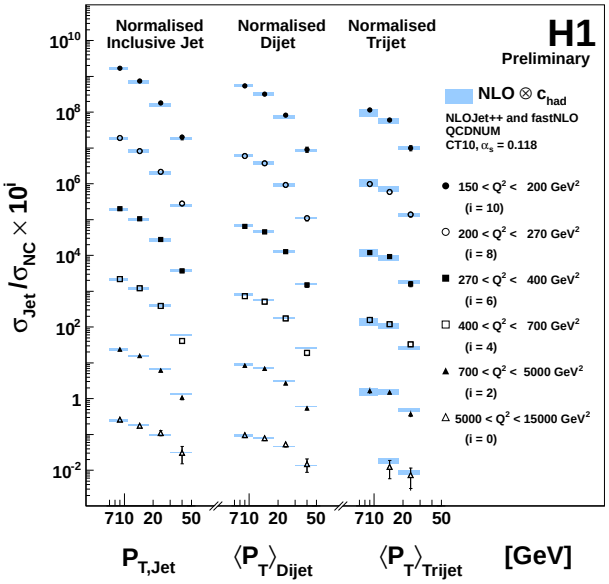

Fig. 5. Normalised inclusive jet,dijet and tri-jet cross sections measured by the H1 Collaboration as a function of the transverse momentum in different Q^2 bins compared to the NLO QCD predictions.

directly takes part in the interaction, whereas the photon acts as a source of partons in events with resolved photoproduction. The ZEUS Collaboration published new double-differential jet cross sections in photoproduction events with a center-of-mass energy of the photon-proton system between 142 and 293 GeV [12]. Compared to DIS measurements, this analysis has a relatively high reach of transverse jet energies, E_T, up to 80 GeV. Overall, a reasonable agreement between data and the NLO predictions (using ZEUS-S PDFs [14] for the proton PDF, GRV-HO for the photon PDF and the programme of Klasen, Kleinwort and Kramer [13]) is observed as shown in Fig. 6. The ZEUS Collaboration has used these jet cross sections to measure $\alpha_s(M_Z)$. The range in $d\sigma/dE_T$ was restricted to $21 < E_T < 71$ GeV in order to reduce potential non-perturbative effects and the impact of the proton PDF uncertainty. An $\alpha_S(M_Z)$ value of

$\alpha_S(M_Z) = 0.1206\ ^{+0.0023}_{-0.0022}$ (exp.) $^{+0.0042}_{-0.0035}$ (th.)

was obtained, where scale uncertainties again represent the dominant uncertainty. The $\alpha_s(M_Z)$ extraction is also performed for various different ranges of E_T^{jet} and this demonstrates the running of α_s within a single experiment, as seen in Fig. 6.

These analyses still have some dependence on the PDF used to predict the jet cross sections. This can be better accounted for by making a simultaneous fit of PDFs and $\alpha_s(M_Z)$. This was done by the HERA experiments by using H1 and

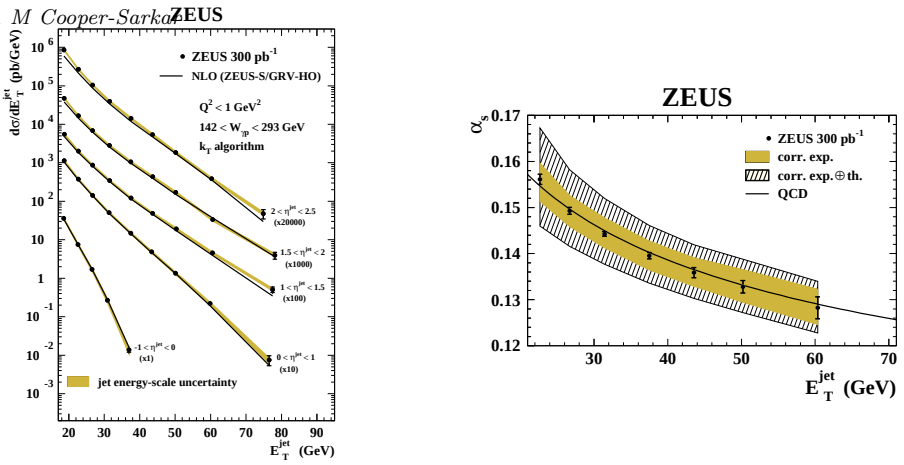

Fig. 6. Left: Inclusive jet cross section in photoproduction measured by the ZEUS Collaboration as a function of the transverse jet energy in different rapidity regions and compared to the NLO prediction. Right: the extracted values of α_s measured for different ranges of E_T^{jet}.

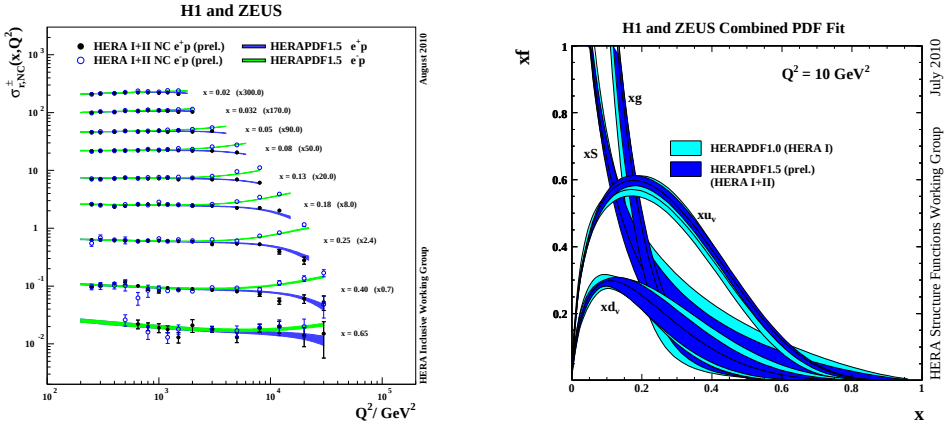

Fig. 7. Left: HERA combined data points for the NC $e^{\pm}p$ cross-sections as a function of Q^2 in bins of x, for data from the HERA-I and II run periods. The HERAPDF1.5 fit to these data is also shown on the plot. Right: Parton distribution functions from HERAPDF1.0 and HERAPDF1.5; xu_v, xd_v,$xS = 2x(\bar{U} + \bar{D})$ and xg at $Q^2 = 10$ GeV^2.

ZEUS jet data together with the combined HERA inclusive data. The preliminary HERA-II data were first combined with the HERA-I data to yield an inclusive data set wih improved accuracy at high Q^2 and high x [5]. This new data set is used as the sole input to a PDF fit called HERAPDF1.5 [7] which uses the same formalism and assumptions as the HERAPDF1.0 fit. Fig. 7 (left) shows the combined data for NC $e^{\pm}p$ cross-sections with the HERAPDF1.5 fit superimposed. The parton distribution functions from HERAPDF1.0 and HERAPDF1.5 are compared in Fig. 7 (right). The improvement in precision at high x is clearly visible.

The HERAPDF1.5 analysis has been extended to include H1 and ZEUS inclu-

sive jet data [15,16,17,18]. The new PDF set which results is called HERAPDF1.6 [8]. For these fits the HERAPDF1.5 parametrisation of the gluon distribution and the valence distribution is extended. This more flexible parametrisation is called HERAPDF1.5f [1]. The extra flexibility does not change the NLO PDFs central values significantly, and the PDF uncertainties are also not much increased.

When the jet data are added the HERAPDF1.6 PDFs are also similar, and there is no tension between the jet data and the inclusive data. For the jet data the NLO cross-sections are caluclatedusing NLOJet+ [10]. The impact of the jet data is clearly seen when $\alpha_S(M_Z)$ is allowed to be a free parameter of the fit. Fig. 8 shows the PDFs for HERAPDF1.5f and HERAPDF1.6, each with $\alpha_S(M_Z)$ left free in the fit. It can be seen that without jet data the uncertainty on the gluon PDF at low x is large. This is because there is a strong correlation between the low-x shape of the gluon PDF and $\alpha_S(M_Z)$. However once jet data are included the extra information on gluon induced processes reduces this correlation and the resulting uncertainty on the gluon PDF is not much larger than it is for fits with $\alpha_S(M_Z)$ fixed.

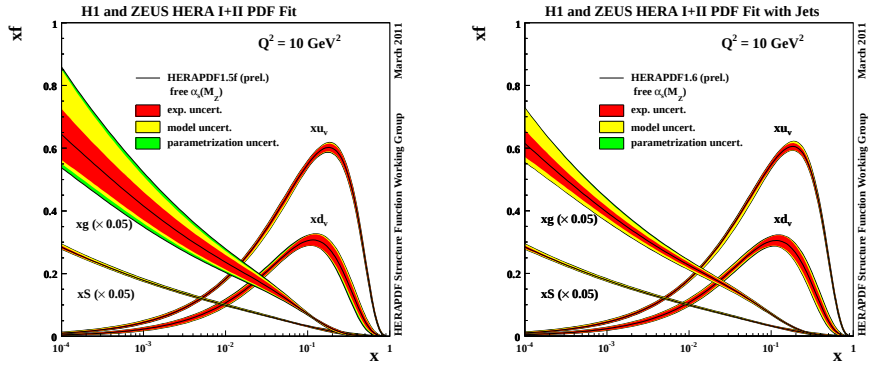

Fig. 8. The parton distribution functions $xu_v, xd_v, xS = 2x(\bar{U} + \bar{D}), xg$, at $Q^2 = 10$ GeV^2, from HERAPDF1.5f and HERAPDf1.6, both with $\alpha_S(M_Z)$ treated as a free parameter of the fit. The experimental, model and parametrisation uncertainties are shown separately. The gluon and sea distributions are scaled down by a factor 20.

Fig. 3.2 shows a χ^2 scan vs $\alpha_S(M_Z)$ for the fits with and without jets, illustrating how much better $\alpha_S(M_Z)$ is determined when jet data are included. The model and parametrisation errors are also much better controlled.

The value of $\alpha_s(M_Z)$ extracted from the HERAPDF1.6 fit is:

$\alpha_S(M_Z) = 0.1202 \pm 0.0013(exp) \pm 0.0007(model/param) \pm 0.0012(had) + 0.0045/-0.0036(scale)$

Model and parametrisation uncertainties on $\alpha_S(M_Z)$ are estimated in the same way as for the PDFs [1] and the uncertainties on the hadronisation corrections applied to the jets are also evaluated. The scale uncertainties are estimated by varying the renormalisation and factorisation scales chosen in the jet publications by a factor

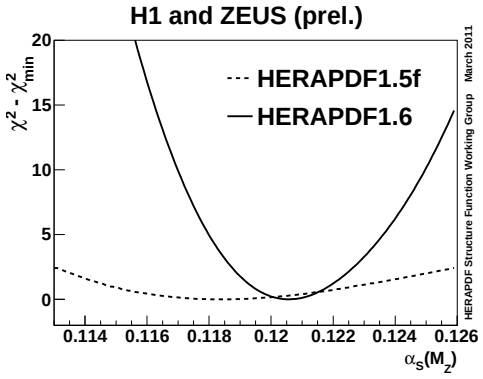

Fig. 9. The difference between χ^2 and its minimum value for the HERAPDF1.5f and HERAPDf1.6 fits as a function of $\alpha_s(M_Z)$

of two up and down. The dominant contribution to the uncertainty comes from the jet renormalisation scale variation.

4. Summary

Charm production data from the HERA experiments ZEUS and H1 have been combined and used to determine the charm quark mass within various heavy quark schemes. Jet cross sections at HERA have been used to determine $\alpha_s(M_Z)$.

References

1. A.M. Cooper-Sarkar, 2012 J.Phys.G **39**, 093001
2. R.S. Thorne and R.G. Roberts, Phys. Lett. B **421**,303 (1998) and hep-ph/0606244
3. F. D. Aaron *et al.* [H1 and ZEUS Collaboration], JHEP **1001** (2010) 109 [arXiv:0911.0884 [hep-ex]].
4. F. D. Aaron *et al.* [H1 and ZEUS Collaboration], 2013 Eur.Phys.J.C**73**2311 [arXiv:1211.1182[hep-ex]].
5. H1 and ZEUS Collaborations, H1prelim-10-141, ZEUS-prel-10-017.
6. S. Alekhin an S. Moch, 2011 Phys.Lett.B**699**345
7. H1 and ZEUS Collaborations, H1prelim-10-142, ZEUS-prel-10-018.
8. H1 and ZEUS Collaborations, H1prelim-11-034, ZEUS-prel-11-001.
9. H1 Collaboration, H1prelim-12-031
10. NLOJEt++, Z Nagy, hep-ph/9605323, hep-ph/0307268
11. H-L. Lai *et al* CT10, arXiv:1007.2241, hep-ph
12. H. Abramowicz *et al*(ZEUS Collaboration) 2012 Nucl.Phys.B**864**1
13. M. Klasen, T. Kleinwort and G. Kramer, 1998 Eur. Phys. J.C**1**1
14. S. Chekanov *et al* (ZEUS Collaboration) 2003 Phys.Rev.D**67** 012007
15. F.D. Aaron *et al* (H1 Collaboration) 2010 Eur.Phys.J.C**65** 363
16. F.D. Aaron *et al* (H1 Collaboration) 2010 Eur.Phys.J.C**67** 1
17. S. Chekanov *et al* (ZEUS Collaboration) 2002 Phys.Lett.B**547** 164
18. S. Chekanov *et al* (ZEUS Collaboration) 2007 Nucl.Phys.B**765** 1